ACS Sustainable Chemistry & Engineering

Research Article

pubs.acs.org/journal/ascecg

Continuous Gas-Phase Synthesis of 1-Ethyl Chloride from Ethyl Alcohol and Hydrochloric Acid Over Al_2O_3-Based Catalysts: The "Green" Route

Natalia Bukhanko,[†] Ajaikumar Samikannu,[†] William Larsson,[†] Andrey Shchukarev,[†] Anne-Riikka Leino,[‡] Krisztian Kordás,[†,‡] Johan Wärnå,[†,§] and Jyri-Pekka Mikkola*[,†,§]

[†]Technical Chemistry, Department of Chemistry, Chemical-Biological Center, Umeå University, SE-90187, Umeå, Sweden

[‡]Microelectronics and Materials Physics Laboratories, University of Oulu, FIN-90570, Oulu, Finland

[§]Laboratory of Industrial Chemistry and Reaction Engineering, Process Chemistry Centre, Åbo Akademi University, Biskopsgatan 8, FIN-20500, Turku/Åbo, Finland

ABSTRACT: The synthesis of 1-ethyl chloride in the gas-phase mixture of ethanol and hydrochloric acid over $ZnCl_2/Al_2O_3$ catalysts was studied in a continuous reactor using both commercial and tailor-made supports. The catalytic materials were characterized by the means of structural (XPS, TEM, XRD, and BET) and catalytic activity (selectivity and conversion) measurements. The reaction parameters such as temperature, pressure, and feedstock flow rates were optimized for the conversion of ethanol to ethyl chloride. The new tailor-made highly porous Al_2O_3-based catalyst outperformed its commercial counterpart by exhibiting high conversion and selectivity (~98%) at the temperature of 325 °C. Long-term stability tests (~240 h) confirmed the excellent durability of the tailor-made alumina catalysts. The process demonstrated here poses an efficient and economic "green" large-scale on-site synthesis of this industrially important reactant in industry, where bioethanol is produced and 1-ethyl chloride is necessary, e.g., for ethylation of cellulose and synthetic polymer products. On-site in situ production of ethyl chloride avoids the problems associated with the transportation and storage of toxic and flammable 1-ethyl chloride.

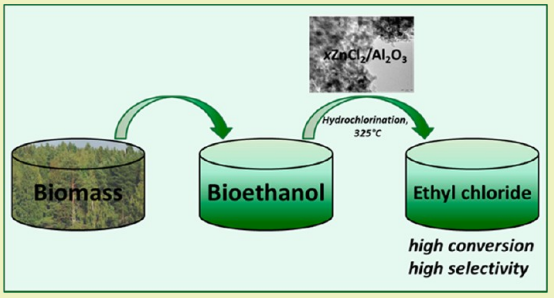

KEYWORDS: *Ethyl chloride, Ethanol, Heterogeneous catalysis, Zinc chloride, High-porosity aluminum oxide*

INTRODUCTION

Ethyl chloride is an important reagent for ethylation reactions used by a number of different industries including cellulose/paper, paint, polymer, and petrochemistry just to mention a few.[1−5] As a halogenated hydrocarbon, having very similar physical−chemical properties to those of freons,[6] ethyl chloride used to be applied as a cooling medium in refrigerants and as la ocal anesthetic to sport injuries.[1] More recently, it was also found useful in the synthesis of ionic liquids.[7,8]

For the bulk synthesis of ethyl chloride, three main industrial approaches are applied. The oldest and least environmentally friendly as well uneconomical ones are the direct hydrochlorination of ethylene and chlorination of ethane on metal chloride catalysts such as $ZnCl_2$, $AlCl_3$, $BiCl_3$, $SbCl_5$, and $FeCl_3$ as well as on their oxychlorides (e.g., $ZrOCl_2$ and BiOCl), optionally supported upon solid carriers such as alumina, silica, or active carbon.[9−17] A more preferred route today is the esterification of alcohols with hydrochloric acid in liquid phase on metal chloride and oxychloride catalyst materials, similar to the processes of methyl chloride synthesis.[18−24] This latter ethanol esterification route may even be considered as "green" because the fossil feedstock can be replaced with bioethanol that can be supplied from renewable resources, such as multi-product lignocellulose biorefinery.[25−28] Lignocellulose is the most abundant renewable organic resource for bioethanol production due to the cost and availability of raw materials. Admittedly, all bioethanol production processes are not too green, and a life cycle analysis (LCA) reveals that, e.g., processes utilizing edible crops (such as corn) are not necessarily the most eco-friendly ones.[29] Nevertheless, the key for reducing the total impact is to integrate a fermentation process to other processes available at state-of-the-art multi-product biorefinery sites. The technology for bioethanol production from biomass has to evolve greatly for an economical commercial-scale utilization of the renewable biomass resources. Consequently, we need to improve our energy availability, decrease air pollution, and diminish atmospheric CO_2 accumulation.[26−28] Besides easier storage and transportation, a further advantage of using ethanol instead of hydrocarbons[9,10,14,17] is its frequently occurring on-site availability at biorefineries, where eventually the largest volumes of ethyl chloride are intended to be used to produce ethyl cellulose and ethyl-hydroxyethyl cellulose for paper and paint components.[5] In general, the process of ethyl chloride synthesis

Received: July 5, 2012
Revised: April 30, 2013
Published: May 20, 2013

from ethanol and hydrochloric acid can be considered as "green" because of high conversion of reagents into products and the absence of hazardous wastes.

The development of ethyl chloride production in continuous reactors with high conversion and selectivity is still a challenging goal in the modern chemical industry. Because of a large volume of produced ethyl chloride (only in the United States 60,000 tons in 1995[23]), a higher conversion and selectivity with optimal reaction temperature and/or catalyst with better durability and safety (without using CCl_4 in feedstock[24] or highly toxic catalysts[18,21,22]) would result in considerable economic and environmental benefits, particularly for ethanol esterification processes. Nevertheless, the most important industrial use of ethyl chloride is in treating cellulose to make ethyl cellulose and related derivatives. Consequently, the use of ethyl chloride has more recently declined in the western world, e.g., due to the closure of many pulping and adjacent cellulose processing industries.[30,31]

In this work, we studied alumina and alumina-supported $ZnCl_2$ catalyst materials in a continuous reactor to produce ethyl chloride from ethanol and hydrochloric acid. The goal of the study was to reveal the effect of catalyst structure on the reaction and to find experimental conditions that can result in similar or better conversion and selectivity than that with commercially available alumina-based catalyst materials. The partially amorphous nanostructured highly porous alumina we synthesized was found to outperform its crystalline counterpart when combined with a $ZnCl_2$ co-catalyst (0−2 wt %). The details of catalyst material structure along with the corresponding catalytic activities are discussed in this paper.

EXPERIMENTAL SECTION

Catalysts Preparation. High-porosity aluminum oxide prepared by the sol−gel method was used as the catalyst support for the materials of group I. The commercial Al_2O_3 (La Roche, A-201, fraction $x < 250$ μm and fraction $250 < x < 500$ μm, named as No. I and No. II, respectively) was used as the supports for the materials of group II. Zinc chloride salt (analytical grade, > 98%, Merck) was used for the preparation of modified catalysts. The reactants, ethyl alcohol (99.5% analytical grade, Solveco) and HCl anhydrous (99.999%, PRAXAIR), were used as received.

The high-porosity Al_2O_3, prepared via solvo-thermal technique starting from aluminum isopropoxide as the aluminum precursor, was used to prepare the catalysts of group I. In a typical procedure, 200 mL of toluene, 2 mL of water, and 22 mL of dry methanol were placed in a 500 mL round-bottomed flask under constant stirring in a temperature-controlled oil bath at 25 °C. The aluminum iso-propoxide dissolved in a mixture of methanol (22 mL) and toluene (30 mL) was added to the above mixture under constant stirring and stirred overnight. The resultant mixture was transferred into a stainless steel autoclave. The autoclave was closed tightly, shortly purged with nitrogen gas, and then pressurized with nitrogen gas to 1 bar. Thereafter, the autoclave temperature was slowly increased to 270 °C with a heating rate of 3 °C/min. After attaining the target temperature, the vapor pressure in the autoclave was immediately released, still trying to maintain a constant temperature. Consequently, the heater was turned off, and the autoclave was removed from the heating mantle and cooled to room temperature. The resultant aero-gel was dried overnight in air at 120 °C. As the next step, the material was calcined under air atmoshpere at 600 °C for 5 h with a heating rate of 1 °C/min. The calcined material was stored in a desiccator.

The modified high-porosity alumina catalysts x wt % $ZnCl_2/Al_2O_3$ ($0 < x < 2$) were prepared by means of an impregnation method. The low concentration of $ZnCl_2$ was desirable in order to avoid any potential agglomeration or pore blockage because $ZnCl_2$ has a rather low melting point.[21] A predetermined amount of freshly prepared aluminum oxide was dispersed in 100 mL of methanol at a constant stirring rate and at room temperature. The calculated amount of $ZnCl_2$ was dissolved in water; the solution was added dropwise to the aluminum oxide suspension under constant stirring and left under stirring for 5 h. Finally, the materials were dried in an oven at 120 °C for 12 h. The $ZnCl_2$ loading was varied as follows: 0.5, 1, 2, and 5 wt % for high-porosity Al_2O_3 support and 2 wt % for the commercial Al_2O_3 (both types I and II).

Catalyst Characterization. The morphology of catalytic materials was examined using LEO 912 OMEGA energy-filtered TEM (transmission electron microscopy) operating at 120 kV.

To describe the quantitative and qualitative surface composition of catalytic materials before and after reaction, the X-ray photoelectron spectroscopy (XPS) technique was used. All XPS spectra were recorded with a Kratos Axis Ultra electron spectrometer equipped with a delay line detector. A monochromated Al Kα source operated at 150 W, hybrid lens system with magnetic lens, analysis area of 0.3 mm × 0.7 mm, and charge neutralizer were used for the measurements. The binding energy scale was referenced to the C 1s line of aliphatic carbon, set at 285.0 eV. Processing of the spectra was accomplished with the Kratos software.

Phase composition of all catalytic materials was analyzed by powder X-ray diffraction (Siemens D5000 XRD, Cu Kα radiation). The recording was carried out for 2Θ angles from 5° to 80° at a scanning speed of 0.5°/min. Diffract-plus EVA database (Bruker) was used for phase composition identification. Crystallite size was calculated by the Scherer equation[32] using the reflections of (400) and (440) planes for γ-Al_2O_3 and the (020) and (021) for AlO(OH) phases.

The pore diameter, pore volume, and surface area of the carbon supports and catalysts were measured at 77 K in a Micromeritics Tristar 3000 surface area and porosity analyzer by the N_2 adsorption−desorption method (nitrogen physisorption). Around 0.2 g sample was degassed at 200 °C for 2 h in 10^{-5} Torr vacuum to remove the moisture from the pores of the material. Pore diameter and pore volume were calculated from the adsorption isotherms using the BJH method. Surface area was calculated using the adsorption data up to a relative pressure of 0.2 by BET method.

Catalytic Experiments. Catalytic reactions were performed in a tailor-made pressurized fixed bed reactor (ID 10 mm, length 260 mm) constructed from stainless steel tube with a tantalum lining inside to eliminate corrosion processes during the reaction. Before each and every reaction, the catalyst was heated overnight (in situ) in the reactor and at the reaction temperature under nitrogen flow. The pretreatment was carried out in order to remove all moisture from the reaction system. The temperature was controlled by separate external heaters along the reactor system. Two thermocouples were placed inside the reactor, well extending up to the catalytic bed and used to monitor the reaction temperature. The catalyst bed consisted of the catalyst of choice (m_{cat} = 0.25 g, l_{bed} = 3 cm) and glass beads as spacers in the reactor. Ethyl alcohol was fed with an HPLC-pump and vaporized at 250 °C before the flow was entering the reactor. The reaction was carried out at different temperatures: 200, 250, 275, 300, and 325 °C, all under atmospheric conditions and under an elevated pressure of 6 bar. Reaction temperatures beyond 325 °C were avoided to counter-effect the formation of excessive amounts of byproducts—long chain alkanes and aromatic hydrocarbons. The molar ratio of feedstock was $n(C_2H_5OH):n(HCl)$ = 1.05:1, 1.025:1, and 1:1. The flow rates of HCl and C_2H_5OH were controlled by means of PC and calibrated before each and every experiment. To remove traces of water and unreacted acid, the mixture of products leaving the reactor was passed through the vessel with the desiccant—calcium oxide (in some cases with the addition of molecular sieves 3A beads)— heated to 100−105 °C.[33,34] The reaction products were collected in a cooling trap system (T = −5 °C, water−ethylene glycole mixture). The samples for analysis were withdrawn every 10 min using the equipment cooled to −5 °C because of the high volatility of ethyl chloride. The liquid-phase products were analyzed using a gas chromatograph (GC, Agilent 6890N) equipped with a flame ionized detector (FID) and HP-PLOT/U capillary column (oven temperature 180 °C, isothermal regime). The conversion was calculated as a ratio

Table 1. BET Surface Area, Pore Size, and Pore Volume Data for the Catalysts Used

	S_{BET} (m^2/g)			pore size (nm)			pore volume (cm^3/g)		
catalyst	fresh	spent (short time)	spent (long time)	fresh	spent (short time)	spent (long time)	fresh	spent (short time)	spent (long time)
Al_2O_3 high porosity	429.1	342.9	245.5	18.0	20.5	17.7	1.9	1.8	1.1
Al_2O_3 No. I	317.8	129.1	73.8	4.5	9.5	13.3	0.4	0.3	0.2
Al_2O_3 No. II	325.0	128.3	72.7	5.0	7.5	12.2	0.4	0.2	0.2
0.5 wt % $ZnCl_2/Al_2O_3$ high porosity	425.4	228.1	–	21.1	21.2	–	2.3	1.2	–
1 wt % $ZnCl_2/Al_2O_3$ high porosity	423.2	225.1	–	18.8	22.1	–	2.0	1.2	–
2 wt % $ZnCl_2/Al_2O_3$ high porosity	400.2	244.9	184.2	6.3	13.4	15.1	0.6	0.8	0.7
2 wt % $ZnCl_2/Al_2O_3$ No. I	312.7	129.1	–	4.4	9.5	–	0.3	0.3	–
2 wt % $ZnCl_2/Al_2O_3$ No. II	293.4	133.7	–	5.2	18.4	–	0.4	0.6	–

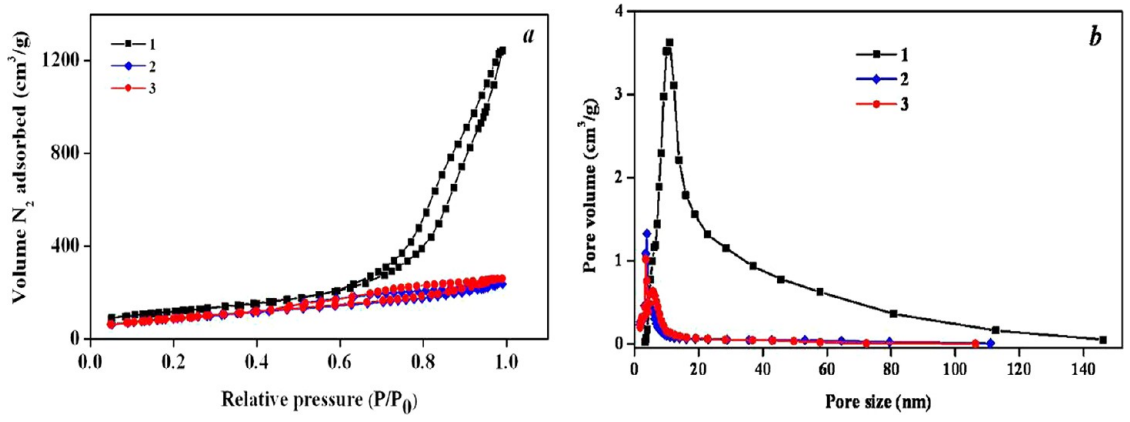

Figure 1. Nitrogen adsorption–desorption isotherms (a) and pore size distribution (b) of different supporting catalytic materials (fresh): 1. high-porosity Al_2O_3, 2. Al_2O_3 No. I, and 3. Al_2O_3 No. II.

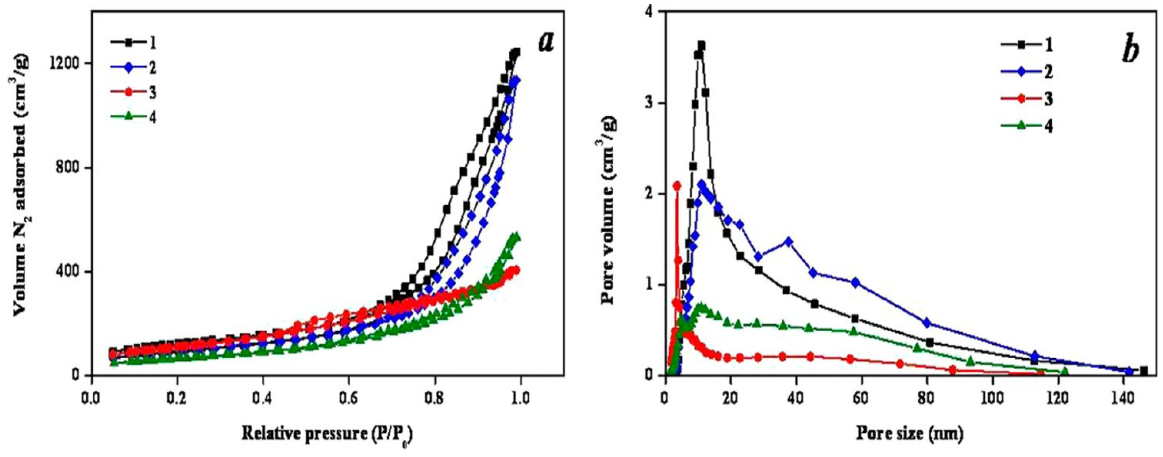

Figure 2. Nitrogen adsorption–desorption isotherms (a) and pore size distribution (b) of the materials: 1. high-porosity Al_2O_3 fresh, 2. high-porosity Al_2O_3 spent, 3. 2 wt % $ZnCl_2/Al_2O_3$ (high porosity) fresh, and 4. 2 wt % $ZnCl_2/Al_2O_3$ (high porosity) spent. The spent catalyst samples were analyzed after 5 h use at 300 °C and p = 6 bar.

of the ethyl chloride moles to the initial molar flow of HCl. The process selectivity was calculated as the ratio between the ethyl chloride amount and the total amount of ethyl chloride as well as diethyl ether formed as a byproduct.

Acid–Base Titration Procedure. Acid–base titration was used to verify the accuracy of the calculations upon conversion of HCl into ethyl chloride (obtained from GC data). The titration procedure was carried out using the 665 Dosimat (Metrohm Swiss made) auto-titrator. The product mixture coming out from the reactor was passed through a 2 M NaOH solution with bromothymol blue indicator (BTB) under constant stirring. The HCl conversion X (%) was calculated using the formula $X = ((1 - n_{(HCl)out})/(n_{(HCl)in})) \times 100$. The value of $n_{(HCl)out}$ was calculated as a ratio $n_{(HCl)in} = ((V_{NaOH} \times C_{NaOH})/t) \times 100$, where V_{NaOH} is the volume of neutralization trap (NaOH solution, mL), C_{NaOH} is the molar concentration of NaOH solution (mol/L), and t denotes the reaction time of NaOH and HCl(s).

RESULTS AND DISCUSSION

Structure and Chemical Composition of Catalyst Materials. Catalysts with various $ZnCl_2$ loading were prepared

dx.doi.org/10.1021/sc300171m | ACS Sustainable Chem. Eng. 2013, 1, 883–893

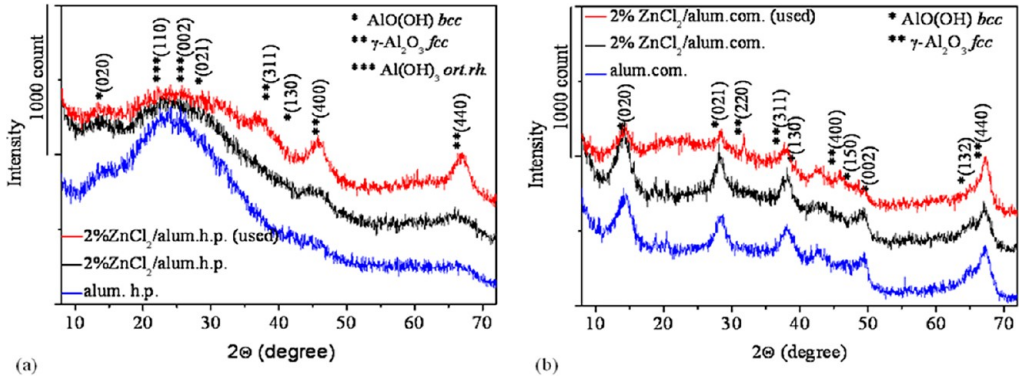

Figure 3. X-ray diffraction patterns of highly porous alumina (a) and commercial Al_2O_3 No. I (b) based catalyst materials. The spent catalyst samples were analyzed after 5 h use at 300 °C and p = 6 bar. Feedstock molar ratios (n_{C2H5OH}: n_{HCl}) of 1:1 and 1.05:1 were applied for the reactions over highly porous and commercial alumina catalyst materials, respectively.

by means of impregnation on different types of aluminum oxides. The techniques such as BET, XRD, TEM, and XPS were used to characterize the catalytic materials.

The results of BET surface area, pore volume, and pore diameter measurements for pure alumina support materials and $ZnCl_2$-impregnated catalysts measured with nitrogen physisorption are given in Table 1. Pure high-porosity alumina exhibited the highest surface area compared to both industrial Al_2O_3 supports. The surface areas for $ZnCl_2$-impregnated high-porosity materials are sligthly lower than for pure support. It can be observed that the commercial Al_2O_3 supports contained substantially lower surface area and pore volume than our high-porosity alumina (Figure 1). Also, the changes in the surface area and pore volume for high-porosity alumina catalysts before and after reaction were studied (Figure 2). It was evident that both the surface area and pore volume decreased substantially during the course of the reaction.. The catalytic materials exhibited very different behavior in terms of surface area decrease. Thus, for tailor-made high-porosity alumina (both for $ZnCl_2$-impregnated and pure), the decrease in surface area was around 20%, whereas for both commercial catalysts, a significantly larger loss of surface area (60%) was observed upon a 5 h run (Table 1). Similar observation was confirmed in the case of long-term experiments (250 h). In summary, the commercial alumina catalysts were much less resistant toward deactivation than the tailor-made alumina, which allows for long-term continuous operations without a catalyst regeneration period. The significant decrease of alumina surface area (both for $ZnCl_2$-impregnated and pure materials) can be explained by blockage of some mesopores following the formation and increasing the crystallinity of new phases AlO(OH), $Al(OH)_3$, and γ-Al_2O_3 on the surface (Figure 3) as well as sintering and coke deposition processes during the reaction.

As assessed by X-ray diffraction analysis, the phase composition and crystal size in the commercial and synthesized highly porous alumina-based catalyst materials had considerable differences (Figure 3a). The pristine $ZnCl_2$-impregnated highly porous materials demonstrated only diffuse reflection suggesting amorphous, or at least very poorly ordered, orthorhombic aluminum hydroxide ($Al(OH)_3$) and *bcc* oxyhydroxide (AlO(OH)) structures in the solid support. After 5 h of use at 300 °C, however, the support undergoes crystallization as the intensity of the amorphous background decreases and at the same time, clear reflections at ~45.9° and ~66.9° 2Θ angles appear corresponding to (400) and (440) planes of the formed γ-Al_2O_3 phase, respectively. From the broadening of the peaks, the average size of the nanocrystals is 3.6 ± 0.6 nm. For spent materials containing 0.5 and 1 wt % $ZnCl_2$, the crystallite sizes are 3.0 and 2.8 nm, respectively. No reflections from any possible phases of $ZnCl_2$ and $AlCl_3$ (in spent samples) were observed.

Significant changes in the phase composition of the alumina support could be observed after long-time experiments at elevated temperature (Figure 4). Thus, for high-porosity

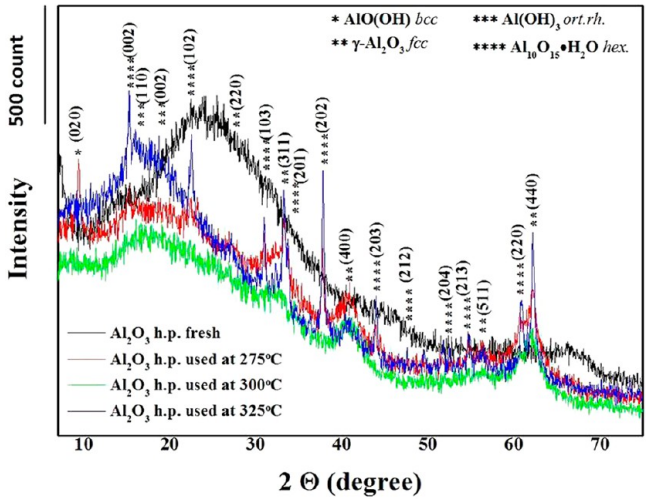

Figure 4. X-ray diffraction patterns of highly porous alumina catalyst materials. The spent catalyst samples were analyzed after using different temperatures, p = 6 bar, and a feedstock molar ratio of n_{C2H5OH}:n_{HCl} = 1:1. The materials spent at 275 and 325 °C were tested during a long time, 124 and 251 h, respectively.

alumina, after prolonged reaction times (124−251 h) at 325 °C, hexagonal phase $Al_{10}O_5{\cdot}H_2O$ was formed. The crystallite size for $Al_{10}O_5{\cdot}H_2O$ was determined to reside at 23.3 ± 6.7 nm and for γ-Al_2O_3 at 3.2 ± 0.2 nm. Interestingly, in case the of spent $ZnCl_2$-impregnated high-porosity materials, the presence of γ-Al_2O_3 and AlO(OH) phases was observed, but the formation of hexagonal phase $Al_{10}O_5{\cdot}H_2O$ was very moderate.

The samples made by using the commercial alumina powder consisted of well-crystallized *bcc* AlO(OH) and γ-Al_2O_3 phases (Figure 3b). For the $ZnCl_2$-impregnated catalyst, the stronger reflection at 31.8° corresponding to the (220) plane of the γ-

dx.doi.org/10.1021/sc300171m | ACS Sustainable Chem. Eng. 2013, 1, 883−893

Al_2O_3 phase was observed. The average size of the AlO(OH) and γ-Al_2O_3 crystallites in the untreated support was measured to be 4.5 ± 0.8 and 5.1 ± 0.1 nm, respectively. These values seem to increase with prolonged use of the catalyst (to 7.3 ± 4.3 and 8.9 ± 2.1 nm, respectively) indicating slight coarsening of the support. Similar to the highly porous alumina-based catalyst, phases $ZnCl_2$ and $AlCl_3$ were not identified in the samples.

Figure 5 (a–d) presents the morphology of the pure high-porosity Al_2O_3 and 2 wt % $ZnCl_2/Al_2O_3$ (high porosity)

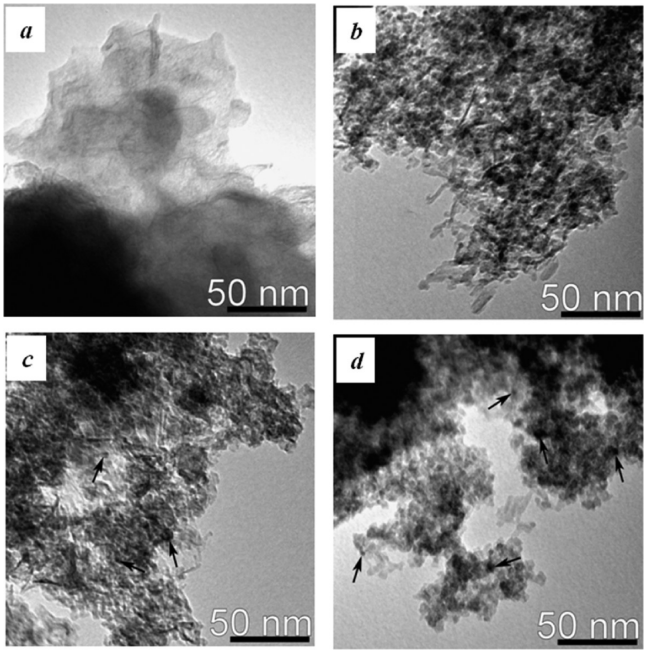

Figure 5. Transmission electron microscopy images of catalytic materials: pure Al_2O_3 (high porosity) fresh (a), pure Al_2O_3 (high porosity) spent (b), 2 wt % $ZnCl_2/Al_2O_3$ (high porosity) fresh (c), and 2 wt % $ZnCl_2/Al_2O_3$ (high porosity) spent (d). The spent samples were analyzed after 5 h use at 300 °C, p = 6 bar, and a molar ratio of n_{C2H5OH}:n_{HCl} = 1:1.

catalysts before and after their use in the reaction. The surface morphology of the catalytic materials, before and after reaction, was analyzed by means of transmission electron microsopy (TEM). It was shown that all high-porosity Al_2O_3 catalysts consisted of nanosized particles with average sizes around 5 nm. The black arrows denote the $ZnCl_2$ particles finely and irregularly distributed on the surface of 2 wt % $ZnCl_2/Al_2O_3$ (high porosity) catalyst. The surface of the spent pure alumina was different from the fresh catalyst and looked more ripe after being used in the reaction (Figure 5). The surface was not substantially altered for the material containing 2 wt % $ZnCl_2$ and was exposed to the reaction environment at 300 and 325 °C. The distribution of $ZnCl_2$ particles on the surface was almost unaffected. The surface of the spent material looks more crystalline than fresh (crystallinity increases with reaction temperature increasing). It is in good agreement with XRD data, indicating the presence of the γ-Al_2O_3 phase in the materials (Figures 3 and 4). The results are similar for the commercial catalysts as well (both pure and $ZnCl_2$-impregnated).

For more information, the XPS analysis was carried out. Both fresh and spent materials were studied. The XPS data are presented in Table 2 as atomic concentration ratios. We conclude that the Al/Zn ratio does not change for the catalyst

Table 2. XPS Data for the Catalysts before and after the Reaction

	atomic concentration ratio		
catalyst	Cl/Al	Al/Zn	Al–OH/Al–O
Al_2O_3 (high porosity) fresh	–	–	0.22
Al_2O_3 (high porosity) spent at T = 325 °C and p atm	0.055	–	0.20
2 wt % $ZnCl_2/Al_2O_3$ (high porosity) fresh	0.024	114.72	0.26
2 wt % $ZnCl_2/Al_2O_3$ (high porosity) spent at T = 325 °C and p atm	0.079	152.24	0.26
2 wt % $ZnCl_2/Al_2O_3$ (No. I) fresh	0.041	82.32	1.09
2 wt % $ZnCl_2/Al_2O_3$ (No. I) spent at T = 300 °C and p = 6 bar	0.073	87.95	0.32

2 wt % $ZnCl_2/Al_2O_3$ (No. I), but the Al–OH/Al–O ratio was decreasing. This indicates that the reaction mechanism should follow the hypothesis of Becerra et al.,[20] i.e., two adjacent sites on the surface might be involved.

Our current hypothesis is that in the case of 2 wt % $ZnCl_2/Al_2O_3$ (high porosity), another reaction mechanism prevails. Because the ratio of Al–OH/Al–O remains constant but the Al/Zn ratio was substantially altered, the single-site reaction model, suggested by Thodos and Stutzman seems plausible.[15] The Al–OH/Al–O ratio for the 2 wt % $ZnCl_2/Al_2O_3$ (high porosity) catalyst was similar to that for pure high-porosity Al_2O_3. In both cases it remained constant. Thus, the reaction might proceed according to the S_{N2} mechanism involving $ZnCl_2$ instead of Al_2O_3.

It was seen that the atomic ratio of Al–OH/Al–O remained constant for the 2 wt % $ZnCl_2/Al_2O_3$ (high porosity) catalyst before and after the reaction, but the Al/Zn ratio was substantially increased. This illustrates the surface depletion of Zn atoms and shows the dominant role of $ZnCl_2$ in the reaction mechanism. The Al–OH/Al–O ratio also remained almost constant for the pure high-porosity Al_2O_3 and was close to that for 2 wt % $ZnCl_2/Al_2O_3$ (high porosity).

For the catalyst 2 wt % $ZnCl_2/Al_2O_3$ (No. I), the atomic ratio Al/Zn was almost unaffected, although the Al–OH/Al–O ratio decreased. Consequently, a surface reaction involving the Al–OH bonds seems to be more dominant that that involving $ZnCl_2$ species.

Catalytic Reaction of Ethanol Hydrochlorination. *Reaction Mechanism and Qualitative Kinetics.* One possible reaction mechanism is proposed and presented in Scheme 1. It illustrates that in the first step the OH^- group of the ethanol molecule is adsorbed on the alumina catalyst surface at the Lewis acid site that leads to weakening of the C–O bond. It makes the second step easier—the nucleophilic attack of C atoms by Cl^- ions with the replacement of the leaving OH^- group according to the S_{N2} mechanism. In the final step, desorption of H_2O molecules adsorbed on catalyst surface occurs. The presence of zinc chloride on the alumina surface leads to an enhancement in the number of acid sites on the surface and, as a sequence, the activity of the catalyst in the reaction. The action of supported $ZnCl_2$ as a Lewis acid catalysis with high product selectivity was shown for some heterogeneous processes: ethylene and higher alkenes hydrochlorination,[17] methyl alcohol hydrochlorination,[21,22] catechol *O*-methylation,[35] and ethene and ethane oxychlorination to

dx.doi.org/10.1021/sc300171m | ACS Sustainable Chem. Eng. 2013, 1, 883–893

Scheme 1. Plausible Reaction Mechanism for Ethanol Hydrochlorination Process Over Al_2O_3 Catalysts

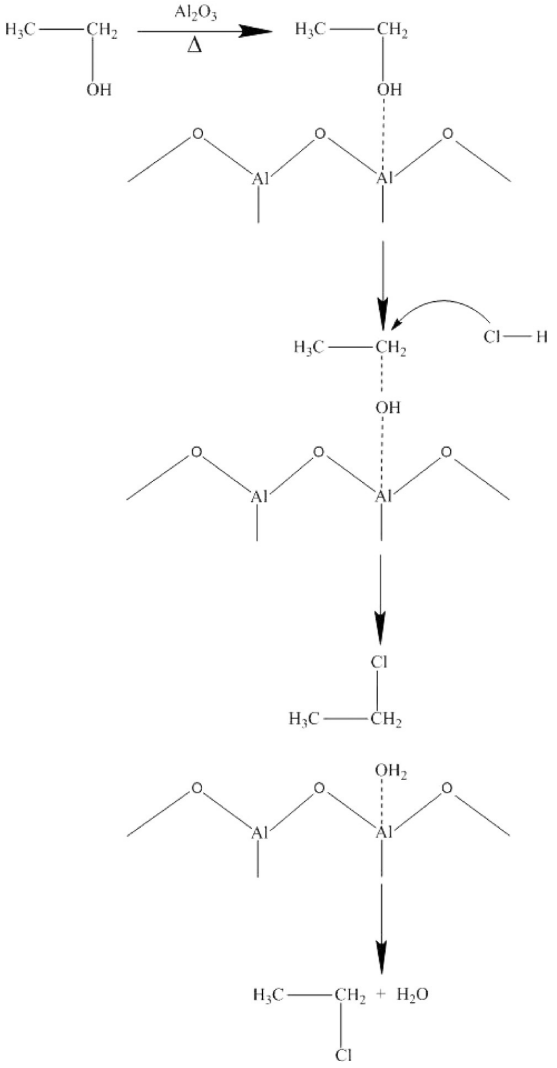

vinyl chloride.[36,37] Svetlanov et al. suggested that a nucleophilic attack can be carried out due to polarization of Cl atoms in HCl as well as by chloride ions of the catalyst.[21] Conte et al. have shown high selectivity of Al_2O_3- and SiO_2-supported Zn^{2+} catalysts for the ethylene hydrochlorination process.[17] The structure of ethanol adsorbed on the alumina catalyst surface (surface ethoxide) was studied earlier.[38−40] The diethyl ether formation is favored with increased surface concentration of the ethoxide, suggesting that a Langmuir−Hinshelwood type of mechanism prevails due to ethoxide pairs on the surface.[36] Topchieva et al. suggested that the surface ethoxide is a reaction intermediate toward ethylene and diethyl ether.[39]

In line with the formalism of Langmuir−Hinshelwood kinetics, simple primary surface reaction steps could be described as follows on Scheme2: A second, plausible Langmuir−Hinshelwood type of kinetic approach was developed for the ethyl alcohol chlorination, and a preliminary regression analysis was conducted in order to find out whether the approach might be a plausible one. The model assumes adsorption of ethanol onto the catalytic site as ethoxy species as well as the hydrochoric acid (steps I, II). As the next step, the adsorbed species can react in two alternative ways. One is via direct interaction with the adjacent molecule (step III) (Scheme 2). Alternatively, in the case when three adjacent sites happen to be occupied by ethoxy species neighbored by an HCl molecule and a proton, diethyl ether may form together with water and ethyl chloride species (step IV) (Scheme 3).

Scheme 2. Simple Mechanistic Approach to Ethanol Hydrochlorination

I	$CH_3CH_2OH + HCl$	← →	$CH_3CH_2Cl + H_2O$
II	$2\ CH_3CH_2OH$	← →	$(CH_3CH_2)_2O + H_2O$
III	$(CH_3CH_2)_2O + HCl$	← →	$CH_3CH_2Cl + CH_3CH_2OH$

Scheme 3. Alternative Mechanistic Approach to Ethanol Hydrochlorination Taking into Account Various Parallell Reactions That We Propose Can Occur

Et: ethanol; Ex: ethoxy; DE: diethyl ether; H2O: water; HCl: hydrochloric acid; H: proton; EtCl: ethyl chloride; HC: hydrocarbon; * Active site

I	Et + **2***	←K1→	**Ex* + H***
II	HCl + *	←K2→	HCl*
III	Ex* + HCl* **+ H***	→r1 (RDS)	EtCl* + **H_2O***
IV	3Ex* + HCl* + **3 H***	→r2 (RDS)	**DE* + $2H_2O$* + EtCl* + ***
V	DE* + HCl*	→r3 (RDS)	EtCl* + Ex*
VI	DE* + H*	→r4 (RDS)	HC* + Ex*
VII	EtCl*	←K3→	EtCl + *
VIII	DE*	←K4→	DE + *
IX	H_2O*	←K5→	H_2O + *
X	HC*	←K6→	HC + *
XI	H*	←K7→	H + *

Consequently, if the adsorbed diethyl ether happens to be in the vicinity of an HCl molecule, yet another ethyl chloride is generated, while an ethoxy species is regenerated onto the surface (step V). On the other hand, if the diethyl ether happens to reside in the vicinity of a proton (from step III), only then will hydrocarbon formation occur together with the regeneration of an ethoxy species (step VI). The remaining steps describe the formalism of the products leaving the active sites on the catalyst surface thus regenerating the sites for a consecutive catalytic round.

Figure 6 demonstrates the mapping of the experimental data to the model data with the help of the Modest software.[41] The software solves the reactor model equations (system of ordinary differential equations) with the backward difference method and optimizes the parameter values using a hybrid method involving Simflex and Levenberg−Marquardt methods. In the regression analysis, reaction steps III−VI were assumed as rate determining ones (RDS). As shown, the results look encouraging, and the full analysis of the kinetics will be published in a forthcoming publication.

Influence of Reaction Parameters and Nature of Catalysts on Conversion. Upon hydrochlorination of ethyl alcohol, 1:1, 1.025:1, and 1.05:1 molar ratios of C_2H_5OH-to-HCl were passed through a fixed catalyst bed (l_{bed} = 3 cm, m_{cat} = 0.25 g). To activate the catalyst surface before reaction and as a consequence to increase the ethyl chloride yield,[21] the HCl flow was turned on at first followed by the ethanol vapor flow (2−3 min later). The conversion was monitored at different temperatures (250, 275, 300, and 325 °C) and pressures (1 and 6 bar). The reaction parameters such as $ZnCl_2$ loading, reaction temperature, pressure, and flow rates were studied in order to obtain better understanding of the ethyl chloride formation process. The duration of experimental runs was

dx.doi.org/10.1021/sc300171m | ACS Sustainable Chem. Eng. 2013, 1, 883−893

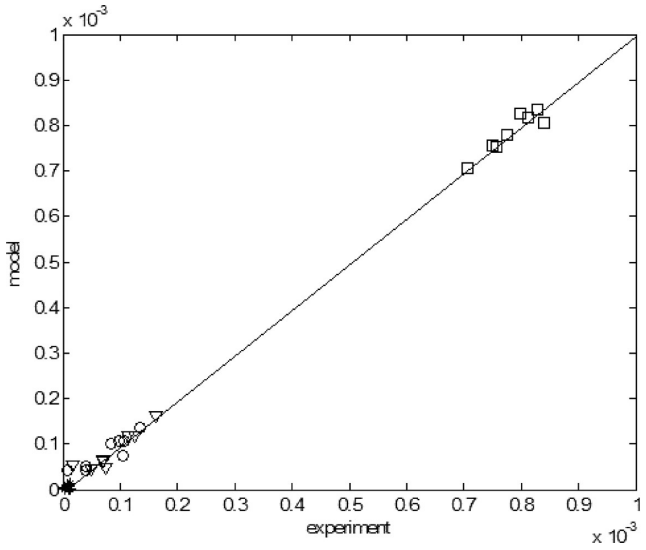

Figure 6. Mapping of the experimental matrix to the model predictions. The experiments were carried out over 2 wt % $ZnCl_2$/Al_2O_3 (high porosity) catalyst.

never less than 6 h for all the experiments. Samples were withdrawn at constant time intervals (10−15 min) and analyzed by means of gas chromatography (GC) and acid−base titration. The conversion values calculated via the titration method were in good agreement with values obtained for GC data for short-time experimental runs (5 h). Some discrepancy in the GC and titration data was observed for several of long-term experiments (>100 h) and could be, probably, explained by presence of bypassed water and traces of ethanol in the CaO trap. All the accessories (syringes, vials) used for sampling procedure had to be properly cooled in order to avoid any losses of the volatile ethyl chloride product. On the basis of careful analysis of the trace compounds found in the chromatograms, besides the desired product (ethyl chloride), minor amounts of diethyl ether as well as traces of ethylene were produced. Table 3 as well as Figures 7 and 8 summarize the conversion and selectivity data for a large set of experiments. The catalytic performance of the non-impregnated high-porosity alumina revealed that the conversion of hydrochloric acid and the selectivity toward ethyl chloride increases with increasing temperature. The conversion of HCl rapidly increased up to 275 °C (91.3%), and a further temperature

Table 3. HCl Conversion and Ethyl Chloride Selectivity Data for Different Catalysts and Reaction Conditions

N	catalyst	*T* (°C)	*p* (bar)	n_{C2H5OH}:n_{HCl}	conversion of HCl (%)	product (C_2H_5Cl) selectivity (%)
1	no catalyst present[a]	325	atm	1:1	19.2	84.3
2	no catalyst present	325	6	1:1	29.3	90.7
3	Al_2O_3 (high porosity)	200	6	1:1	89.6	97.5
4	Al_2O_3 (high porosity)	250	6	1:1	81.4	97.3
5	Al_2O_3 (high porosity)	275	6	1:1	91.3	97.4
6	Al_2O_3 (high porosity)	300	6	1:1	91.3	97.3
7	Al_2O_3 (high porosity)	325	6	1:1	95.2	98.9
8	Al_2O_3 (high porosity)	300	6	1.05:1	93.4	96.6
9	Al_2O_3 (high porosity)	325	6	1.05:1	98.3	98.3
10	Al_2O_3 (high porosity)	325	atm	1:1	95.9	98.1
11	Al_2O_3 (high porosity)	325	atm	1.05:1	95.3	100
12	Al_2O_3 (high porosity)	325	6	1.025:1	98.0	98.4
13	0.5 wt % $ZnCl_2/Al_2O_3$ (high porosity)	300	6	1:1	86.6	96.7
14	1 wt % $ZnCl_2/Al_2O_3$ (high porosity)	300	6	1:1	87.6	96.7
15	2 wt % $ZnCl_2/Al_2O_3$ (high porosity)	300	6	1:1	92.4	97.4
16	0.5 wt % $ZnCl_2/Al_2O_3$ (high porosity)	300	6	1.05:1	91.5	96.0
17	1 wt % $ZnCl_2/Al_2O_3$ (high porosity)	300	6	1.05:1	86.1	94.5
18	2 wt % $ZnCl_2/Al_2O_3$ (high porosity)	300	6	1.05:1	92.9	96.1
19	2 wt % $ZnCl_2/Al_2O_3$ (high porosity)	200	6	1:1	81.3	96.3
20	2 wt % $ZnCl_2/Al_2O_3$ (high porosity)	250	6	1:1	85.6	97.1
21	2 wt % $ZnCl_2/Al_2O_3$ (high porosity)	275	6	1:1	90.8	99.2
22	2 wt % $ZnCl_2/Al_2O_3$ (high porosity)	325	6	1:1	94.7	99.1
23	2 wt % $ZnCl_2/Al_2O_3$ (high porosity)	325	6	1.05:1	91.7	96.6
24	2 wt % $ZnCl_2/Al_2O_3$ (high porosity)	325	atm	1.05:1	92.7	98.1
25	Al_2O_3 (No. I)	250	6	1:1	79.8	98.0
26	Al_2O_3 (No. I)	275	6	1:1	87.0	98.5
27	Al_2O_3 (No. I)	300	6	1:1	75.2	96.2
28	Al_2O_3 (No. I)	325	6	1:1	90.5	96.9
29	2 wt % $ZnCl_2/Al_2O_3$ (No. I)	300	6	1:1	84.1	97.7
30	2 wt % $ZnCl_2/Al_2O_3$ (No. I)	300	6	1.05:1	70.7	96.4
31	Al_2O_3 (No. II)	250	6	1:1	81.6	97.6
32	Al_2O_3 (No. II)	275	6	1:1	93.3	97.7
33	Al_2O_3 (No. II)	300	6	1:1	93.0	97.8
34	Al_2O_3 (No. II)	325	6	1:1	96.1	98.0
35	2 wt % $ZnCl_2/Al_2O_3$ (No. II)	300	6	1:1	88.4	96.5

[a] C_2H_5OH 95 vol % was used as a reactant.

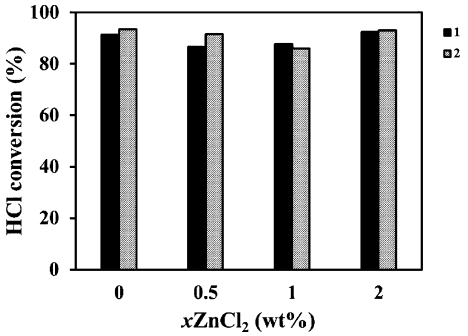

Figure 7. $ZnCl_2$ concentration dependence of HCl conversion for x% $ZnCl_2/Al_2O_3$ (high porosity) at different feedstock molar ratios: 1. n_{C2H5OH}:n_{HCl} = 1:1 and 2. n_{C2H5OH}:n_{HCl} = 1.05:1. The reaction conditions are T = 300 °C and p = 6 bar.

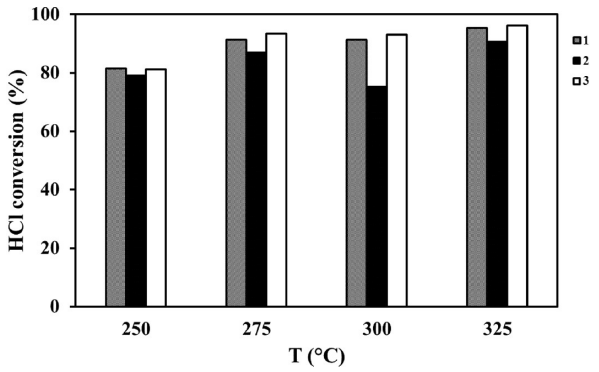

Figure 8. Temperature dependence of HCl conversion over pure alumina catalysts: 1. Al_2O_3 (high porosity), 2. Al_2O_3 No. I, and 3. Al_2O_3 No. II. The reaction conditions are p = 6 bar and a molar ratio of n_{C2H5OH}:n_{HCl} = 1:1.

increase still increases the conversion, yielding 98.3% maximum at 325 °C. As shown, pure high-porosity alumina (entries 9, 12) gives the best conversion and selectivity, both exceeding 98%. Interestingly, the performance was improved by a slight rise in the system pressure (6 bar). In the case when no catalyst was present, the reaction experiment was performed at both pressurized (6 bar) and atmospheric conditions. In most of the experiments, the ethyl alcohol feed was initiated at first, and the reactor setup was allowed to condition for a period of 30 min. This mode of operations avoided the release of highly corrosive HCl into the neutralization bath. Nevertheless, when initating the HCl flow at first and only then starting the ethanol feed, the glass beads packed in the flow reactor were already surface modified by the HCl and were able to act as "poor" catalysts thus giving suprisingly prominent conversion (19% at atmospheric conditions, Table 3).

The catalytic activity of the tailor-made high-porosity alumina was compared with both commercial aluminas (Al_2O_3 No. I and No. II). The reactions were carried out under the same conditions as before, and the results are presented in Table 3. As shown, the nature of the catalytic material significantly influences the system performance. Among the catalysts examined, high-porosity Al_2O_3 exhibited better performance, both in terms of conversion and selectivity toward the formation of ethyl chloride. This difference in catalytic activity can be explained by different phase composition for both of commercial and high-porosity alumina catalysts. Thus, in both commercial catalysts, the presence of the α-phase is revealed, this not being present in the high porosity alumina-based catalysts. The catalytic activity of the α-phase in the ethanol hyrdochlorination process is much lower than that of γ-phase because of the much smaller number of Lewis acid sites on the surface and a greater tendency for $Al(OH)_3$ formation. On the contrary, γ-alumina phase contains a large number of Lewis acid sites on the surface and also is more resistant to interaction with water molecules and possesses a lower tendency for $Al(OH)_3$ formation.

To examine the influence of feed ratio on the conversion and process selectivity, two different feed stock ratios were chosen, n_{C2H5OH}:n_{HCl} = 1:1 and 1.05:1. The experiments were carried out over the pure alumina catalysts as well as the $ZnCl_2$ loaded ones. The results are listed in Table 3. It is revealed that in the case of the excess alcohol, the increasing HCl conversion was observed, but the selectivity was decreased for all catalysts and temperatures due to the higher formation rate of diethyl ether as a byproduct.

Inspired by the earlier investigations and literature data,[17] we proceeded to study whether a metal chloride would enhance the catalytic performance. The enhancement of acidity of the alumina catalyst surface by $ZnCl_2$ loading to improve the conversion and selectivity was the main goal. However, the results of the experiments showed that the use of impregnated catalyst leads to lower conversion than with pure alumina at the same temperatures (Table 3). Thereby, we can conclude that pure alumina has sufficient surface acidity leading to highest conversion. As shown in Table 3 and Figure 7, at equimolar reactant feed, the $ZnCl_2$ addition was not beneficial. However, if an excess of ethyl alcohol was present, the conversions were dramatically improved. The likely underlying reason is the enhanced formation of diethyl ether contributing to more ethyl chloride formation via the secondary route.[21,22]

In order to study the influence of the reaction time and temperature on ethanol hydrochlorination, the reaction was carried out at various temperatures. The results of these experiments are presented in Figure 8. The high temperature (325 °C) experiments were carried out both under atmospheric and elevated pressures (6 bar). It is interesting that the results for commercial alumina No. II are similar to high-porosity alumina, but for alumina No. I, the conversion was not so high at low temperatures (250−300 °C). The results are similar for all the catalysts only at the highest temperature of 325 °C. It was observed that the HCl conversion and ethyl chloride product selectivity increased with a temperature increase. Thus, it can be concluded that the temperature of 325 °C results in the best HCl conversion and the maximum selectivity toward ethyl chloride (98.3% in the case of pure alumina and equimolar feed virtually 100% when a slight excess of ethanol was present in the feed). It was also shown that the pressure effect is very marginal and cannot significantly improve the conversion and selectivity (Table 3).

Calculation of Activation Energy. The reaction rate constant and activation energy of the ethanol hydrochlorination process were calculated using our new simple ethanol hydrochlorination model. The ideal plug flow model, described by Salmi and Wärnå,[42] was used to model the catalytic packed bed reactor

$$\frac{d\dot{n}_i}{dx} = r_i m_{cat}$$

where $\dot{n}_i$ is the molar flow of i-component (mol/min), r_i is the component generation rates (mol/min), and m_{cat} is the catalyst

dx.doi.org/10.1021/sc300171m | ACS Sustainable Chem. Eng. 2013, 1, 883−893

mass (g) in the reactor. The diffusion coefficient *Di* was calculated by using of semi-empirical Fuller–Schettler–Giddings equation[43] and was 5.8×10^{-6} m^2/s. The values of Thiele modulus ϕ and effectiveness factor η were calculated using the model for first-order reaction, described in the literature[43] and the values were 0.08 and 0.99, respectively. Thereby, it was shown that under these experimental conditions the kinetic regime of the reaction of ethanol hydrochlorination is observed.

The results of the E_a calculation are presented for the experiments with non-impregnated and zinc chloride-impregnated Al_2O_3 (high porosity) catalysts in Figure 9, and the values

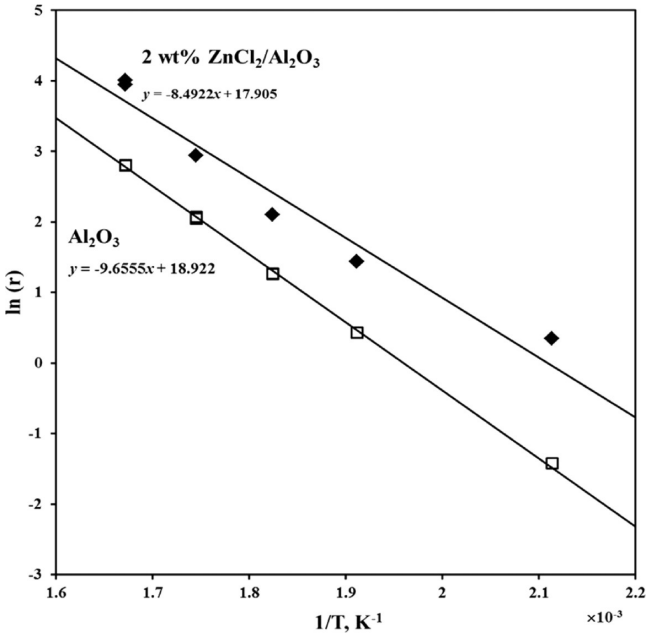

Figure 9. Arrhenius plot for the ethanol hydrochlorination reaction over pure Al_2O_3 and 2 wt % $ZnCl_2/Al_2O_3$ (high porosity) catalysts. The reaction conditions are p = 6 bar and $n_{C2H5OH}:n_{HCl}$ = 1:1.

obtained were estimated to be around 80 and 71 kJ/mol, respectively. Thus, it is evident that $ZnCl_2$ loading to pure alumina significantly lowers the activation energy. The activation energy found for methanol hydrochlorination (90 kJ/mol) reported by Ivanov and Makhlin[44] was in line with the values found for ethanol hydrochlorination as expected.

Long-Time Catalyst Stability Test. The catalyst lifetime is a very important characteristics of any catalytic process. The experiments were performed as follows. During the first 5 h, sampling occurred every 10 min; further, the samples were taken every 2 h and every 10 h after 50 h of reaction time. The total reaction time was more than 200 h. The results are depicted in Figures 10 and 11, respectively. It was observed that the reaction at 275 °C, over non-impregnated high-porosity alumina, gives the HCl conversion of 91.3% coinciding with the selectivity reaching 97.4% during the first 5 h. Furthermore, the conversion was maintained at about 88– 90% throughout the time-on-stream and gradually decreased after 100 h. It should be noted that only one byproduct, diethyl ether, was detected (and traces of hydrocarbons upon some high-temperature experiments). At the temperature of 325 °C, for pure high-porosity alumina, full conversion was approached, and the selectivity obtained remained constant (>98%) throughout the whole experimental time (>200 h). In the case of the $ZnCl_2$-

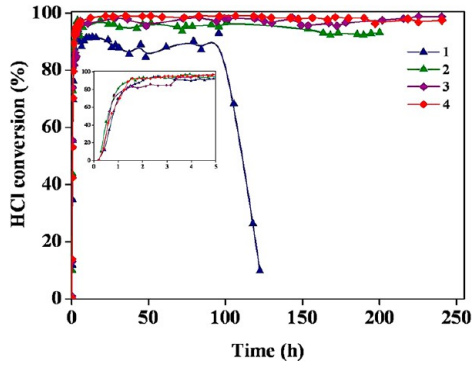

Figure 10. Conversion of HCl into C_2H_5Cl over catalysts: 1. pure Al_2O_3 (high porosity) at 275 °C, 2. pure Al_2O_3 (high porosity) at 325 °C, 3. 2 wt % $ZnCl_2/Al_2O_3$ (high porosity) at 275 °C, and 4. 2 wt % $ZnCl_2/Al_2O_3$ (high porosity) at 325 °C. The reaction conditions are p = 6 bar and $n_{C2H5OH}:n_{HCl}$ = 1:1.

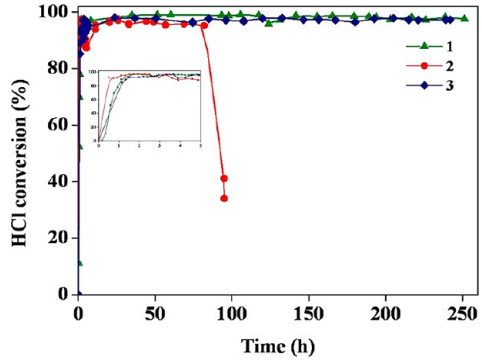

Figure 11. Conversion of HCl into C_2H_5Cl over catalysts: 1. pure Al_2O_3 (high porosity), 2. pure Al_2O_3 (No. I), and 3. pure Al_2O_3 (No. II). The reaction conditions are T = 325 °C, p = 6 bar, and $n_{C2H5OH}:n_{HCl}$ = 1:1.

impregnated version, the results were comparable, although the performance was stable and equally good at a significantly lower temperature of 275 °C. Nevertheless, we should not forget the danger of loss of rather low-melting and thus volatile metal halides, and consequently, their use should be avoided.

CONCLUSIONS

The reaction of ethyl chloride synthesis from ethyl alcohol and HCl over x wt % $ZnCl_2/Al_2O_3$ ($0 < x < 2$) catalysts was studied. Three types of alumina supports, both commercial and tailor made, were investigated. The selectivity and conversion for the catalytic ethanol hydrochlorination over different catalysts were determined. The reaction parameters such as temperature, pressure, and feedstock flow rates were studied upon search for the optimal conversion of ethanol into ethyl chloride. The nature of the alumina catalyst was found to have a significant influence on the reaction performance, and the metal chloride addition to the catalyst structure renders materials with significantly improved "low-temperature" catalytic performance, though any metal chloride fumes potentially emerging are harmful. The tailor-made high-porosity Al_2O_3 was found to be the optimal catalyst exhibiting high conversion (95.3–98.3%) and selectivity of 98.3–100% over extended time periods. Also, it was shown that the activation energy E_a decreased upon $ZnCl_2$ loading into pure high-porosity alumina from 80 to 71 kJ/mol, respectively. Interestingly, the metal chloride addition was not particularly beneficial as long as the molar ratio of the

alcohol and HCl was rigorously kept at 1:1. The lifetime of pure high-porosity alumina was examined in a long-time run. It was shown that conversion and product selectivity were stable during a very long time (>200 h), provided that the reaction temperature was sufficient.

AUTHOR INFORMATION

Corresponding Author

*E-mail: jyri-pekka.mikkola@chem.umu.se; jpmikkol@abo.fi. Tel: +46 90 786 5000.

Notes

The authors declare no competing financial interest.

ACKNOWLEDGMENTS

Financial support from Kempe Foundations (Kempe Stiftelserna) and Bio4Energy Programme are gratefully acknowledged. This work is also associated with the research programmes by the Academy of Finland as well as the Finnish Agency for Innovation and Technology (TEKES).

REFERENCES

(1) *Summary of Emissions Associated with Sources of Ethyl Chloride*; EPA-450/3-88-005; Emissions Standards Division, Office of Air and Radiation, Office of Air Quality Planning and Standards, U.S. Environmental Protection Agency: Research Triangle Park, NC, June 1988, pp 3.1−3.16.

(2) Savage, A. B.; Young, A. E.; Maser, A. T. In *Cellulose and Cellulose Derivatives*; Ott, E., Ed.; Interscience Publishers, Inc.: New York, ; p 913.

(3) Standen, A., Ed.; *Kirk-Othmer Encyclopedia of Chemical Technology*, 2nd ed.; Interscience Publishers, Inc.: New York, 1964; Vol. *4*, pp 638−642.

(4) Considine, D. M., Ed.; *Chemical and Process Technology Encyclopedia*; McGraw-Hill Book Company: New York, 1974, pp 427−429.

(5) Karlson, L.; Olsson, M.; Boström, G.; Piculell, L. Influence of added surfactant on particle flocculation in waterborne polymer−particle systems. *J. Coat. Technol. Res.* **2008**, *5*, 447−454.

(6) Chickos, J. S.; Acree, W. E. Enthalpies of vaporization of organic and organometallic compounds, 1880−2002. *J. Phys. Chem. Ref. Data* **2003**, *32*, 519−878.

(7) Holbrey, J. D.; Seddon, K. R.; Wareing, R. A simple colorimetric method for the quality control of 1-alkyl-3-methylimidazolium ionic liquid precursors. *Green Chem.* **2001**, *3*, 33−36.

(8) Nishimura, K.; Ioroi, K.; Matsui, K. Manufacturing Method of Akylimidazloium Halide. Japanese Patent 2010024153 A, 2010.

(9) Cherniavsky, A. J. Ethyl Chloride Production. U.S. Patent 2807656, Shell Development Company, 1957.

(10) Brown, D. Preparation of Ethyl Chloride. U.S. Patent 3345421, Halcon International, Inc., 1967.

(11) Markish, I.Kh.; Groshev, G. L.; Bulina, N. N.; Kolesnikov, V.Ya.; Vilkov, V. N.; Makarova, T. N. Process for Preparing Ethylene Chloride. Bulletin No. 39, S.U. Patent 1049465 A, 1983.

(12) Golubev, Yu. D.; Shevnina, V. E.; Sporova, L. G. Method of Preparing Catalyst Complex for Ethyl Chloride Synthesis. Bulletin No. 38, S.U. Patent 1047507 A, 1983.

(13) Roush, W. E.; Morell, W. B. Preparation of Ethyl Chloride. U.S. Patent 2110141, The Dow Chemical Company, 1938.

(14) Bond, D. C.; Savoy, M. Preparation of Ethyl Halides. U.S. Patent 2412550, The Pure Oil Company, 1946.

(15) Thodos, G.; Stutzman, L. F. Reaction kinetic studies. Synthesis of ethyl chloride. *Ind. Eng. Chem.* **1958**, *50*, 413−416.

(16) Nagiev, M. F.; Kulieva, V. G.; Mamedova, A. D.; Mirzoyan, N. M. Kinetic study of the process intensification ways of heterogeneous catalytic synthesis of ethyl chloride. *Azer. Him. Zhurn.* **1965**, *4*, 45−50 (in Russian).

(17) Conte, M.; Davies, T.; Carley, A. F.; Herzing, A. A.; Kiely, C. J.; Hutchings, G. J. Selective formation of chloroethane by the hydrochlorination of ethene using zinc catalysts. *J. Catal.* **2007**, *252*, 23−29.

(18) Daudt, H. W. Organic Halides. U.S. Patent 2016075, E.I. du Pont de Nemours & Company, 1935.

(19) Venuto, P. B.; Givens, E. N.; Hamilton, L. A.; Landis, P. S. Organic reactions catalyzed by crystalline aluminosilicates: V. Dehydrohalogenation and related reactions. *J. Catal.* **1966**, *6*, 253−262.

(20) Becerra, A. M.; Castro Luna, A. E.; Ardissone, D. E.; Ponzi, M. I. Kinetics of the catalytic hydrochlorination of methanol to methyl chloride. *Ind. Eng. Chem. Res.* **1992**, *31*, 1040−1045.

(21) Svetlanov, E. B.; Flid, R. M.; Gareeva, D. A. Studies of the catalytic interaction of hydrogen chloride and methanol. I. The kinetics of vapor-phase interaction of methanol and hydrogen chloride. *Russ. J. Phys. Chem.* **1966**, *40*, 2302−2308 (in Russian).

(22) Svetlanov, E. B.; Flid, R. M. Studies on the field of catalytic interaction of hydrogen chloride and methanol. II. The kinetics of reactions of methanol dehydration and dimethyl ether hydrochlorination over catalysts in methyl chloride vapor-phase synthesis. *Russ. J. Phys. Chem.* **1966**, *40*, 3055−3059 (in Russian).

(23) Weissermel, K.; Arpe, H.-J. *Industrial Organic Chemistry*, 4th ed.; Wiley-VCH: Weinheim, Germany, 2003.

(24) McCrudy, J. L. Continuous Process for the Manufacturing of Ethyl Chloride. U.S. Patent 2516638, The Dow Chemical Company, 1950.

(25) Zhang, Y.-H. P.; Ding, S.-Y.; Mielenz, J. R.; Cui, J.-B.; Elander, R. T.; Laser, M.; Himmel, M. E.; McMillan, J. R.; Lynd, L. R. Fractionating recalcitrant lignocellulose at modest reaction conditions. *Biotechnol. Bioeng.* **2007**, *97*, 214−223.

(26) Prasal, S.; Singh, A.; Joshi, H. C. Ethanol as an alternative fuel from agricultural, industrial and urban residues. *Resour., Conserv. Recycl.* **2007**, *50*, 1−39.

(27) Kim, S.; Dale, B. E. Global potential bioethanol production from wasted crops and crop residues. *Biomass Bioenergy.* **2004**, *26*, 361−375.

(28) Soccol, C. R.; Faraco, V.; Karp, S.; Vandenberghe, L. P. S.; Thomaz-Soccol, V.; Woiciechowski, A.; Pandey, A. Lignocellulosic Bioethanol: Current Status and Future Perspectives. In *Biofuels: Alternative Feedstocks and Conversion Processes*; Academic Press: San Diego, 2011; Chapter 5, pp 101−122.

(29) Baral, A.; Bakshi, B. R.; Smith, R. L. Assessing resource intensity and renewability of cellulosic ethanol technologies using eco-LCA. *Environ. Sci. Technol.* **2012**, *46*, 2436−2444.

(30) Forest Industries - Skogsindustrierna. http://www.forestindustries.se (accessed January 10, 2012).

(31) Finnish Forest Industry. http://www.forestindustries.fi (accessed January 9, 2012).

(32) Scherrer, P. Bestimmung der grösse und der inneren struktur von kolloidteilchen mittels röntgenstrahlen. *Göttinger Nachrichten.* **1918**, *2*, 98−100.

(33) Burfield, D. R.; Smithers, R. H. Desiccant efficiency in solvent and reagent drying. 7. Alcohols. *J. Org. Chem.* **1983**, *48*, 2420−2422.

(34) Kimball, R. H.; Jefferson, G. D.; Pike, A. B. *Organic Synthesis*; Wiley: New York, 1943; Collect. Vol. *II*, p 284.

(35) Fu, Z.; Yu, Y.; Yin, D.; Xu, Y.; Liu, H.; Liao, H.; Xu, Q.; Tan, F.; Wang, J. Vapor-phase highly selective *O*-methylation of catechol with methanol over $ZnCl_2$ modified γ-Al_2O_3 catalysts. *J. Mol. Catal. A: Chem.* **2005**, *232*, 69−75.

(36) Lemanski, M. F.; Leitert, F. C.; Vinson, C. G. Catalyst and Process for Production of VCM. U.S. Patent 4115323, Diamond Shamrock Corporation, 1978.

(37) Pritchett, E. G. Process for Preparing Unsaturated Chlorohydrocarbons and Saturated Polychlorohydrocarbons by Oxychlorination of Hydrocarbons and Catalyst System Therefor. U.S. Patent, 3720723, National Distillers and Chemical Corporation, 1973.

(38) Arai, H.; Take, J.; Saito, Y.; Yoneda, Y. Ethanol dehydration on alumina catalysts. I. The thermal desorption of surface compounds. *J. Catal.* **1967**, *9*, 146−153.

(39) Topchieva, K. V.; Yun-Pin, K.; Smirnova, I. V. 81 function of surface compounds in the study of catalytic dehydration of alcohols over aluminum oxide and silica-alumina catalysts. *Adv. Catal.* **1957**, *9*, 799−806.
(40) Pines, H.; Manassen, J. The mechanism of dehydration of alcohols over alumina catalysts. *Adv. Catal.* **1966**, *16*, 49−92.
(41) Haario, H. *MODEST User's Guide*; Profmath Oy: Helsinki, 2007.
(42) Salmi, T.; Wärnå, J. Modelling of catalytic packed-bed reactors: Comparison of different diffusion models. *Comput. Chem. Eng.* **1991**, *15*, 715−727.
(43) Salmi, T. O.; Mikkola, J.-P.; Wärnå, J. P. Catalytic Two-Phase Reactions. In *Chemical Reaction Engineering and Reactor Technology*; CRC Press: Boca Raton, FL, 2010; p177−178.
(44) Ivanov, S. I.; Makhlin, V. A. Catalytic interaction of methanol with hydrogen chloride on γ-Al_2O_3: Kinetics and mechanism of the reaction. *Kinet. Catal.* **1996**, *37*, 812−818.